Remote Effect of the Model Cold Bias in the Tropical North Atlantic on the Warm Bias in the Tropical Southeastern Pacific

Liping Zhang[1], Chunzai Wang[2], Zhenya Song[3] and Sang-Ki Lee[1 & 2]

[1] Cooperative Institute for Marine and Atmospheric Studies
University of Miami
Miami, Florida

[2] NOAA Atlantic Oceanographic and Meteorological Laboratory
Miami, Florida

[3]The First Institute of Oceanography, State Oceanic Administration, Qingdao, China.

Submitted to GRL

Dec 2013

Abstract

Most state-of-the-art climate models show significant systematic biases in the tropical southeastern Pacific (SEP) and tropical North Atlantic (TNA). These biases manifest themselves as the sea surface temperature (SST) in the SEP being too warm and the SST in the TNA being too cold. That is, as the cold SST biases appear in the TNA, the warm SST biases also occur in the SEP. This indicates that if climate models cannot succeed in simulating the TNA variability, they will also fail at least partially in the SEP. Our coupled model experiments show that the cold SST bias in the TNA results in a weakening of the Hadley-type circulation from the TNA to the SEP. This meridional circulation reduces the South Pacific subtropical anticyclone and the associated subsidence, which in turn leads to a reduction of low clouds, a weakening of the easterly trade wind and thus an increase of the warm SST bias in the SEP.

1. Introduction

The large asymmetry of SST about the equator is one of the most striking climate features in the eastern tropical Pacific. In this region SST is higher to the north and lower to the south throughout the seasonal cycle. In association with the relatively cool SST, the SEP is characterized by large-scale subsidence, extensive and persistent stratocumulus clouds. However, most climate models fail to reproduce the observed seasonal cycle in the eastern tropical Pacific [*Szoeke and Xie*, 2008; *Mechoso et al.*, 1995]. One of the most common errors in climate models is a warm SST bias in the SEP, with the warm bias extending thousands of kilometers off the coast of Peru. The warm SST bias in the SEP may have multiple sources. One is the shortage of model low-level stratus clouds in the region, so that an excessive amount of solar radiation reaches the sea surface [*Ma et al*., 1996; *Meehl et al*., 2005]. Near the South American coast, warm SSTs could be associated with weak coastal upwelling due to the underestimation of alongshore surface winds [*Huang and Schneider*, 1995; *Schneider et al*., 1997]. Furthermore, current ocean GCMs do not have high enough resolution to resolve vigorous mesoscale eddies which spread the cold signals from the coastal upwelling zone into the open ocean [*Colbo and Weller*, 2007]. Overall, previous studies primarily focus on the local influence on the SST bias in the SEP.

Wang et al. [2010] suggested that there is an interhemispheric influence of the Atlantic Warm Pool (AWP) on the SEP. They pointed out that an anomalously large (small) AWP during the boreal summer results in a strengthening (weakening) of the Hadley-type circulation with enhanced descent (ascent) over the SEP. Climate models in CMIP5 further show that virtually all of coupled models have significant, but synchronous biases in the SEP and TNA Oceans (Fig. 1). These biases manifest themselves as the SST in the SEP Ocean being too warm and SST in the TNA being too cold. The magnitude of these biases can be as large as 3°C or more, resulting in a significant distortion of the coupled annual cycle of the tropical eastern Pacific and Atlantic in these models. Given the magnitude of these biases and the interhemispheric influence of the AWP on the SEP, an interesting question arises: Is it possible that the warm bias in the SEP may be attributed, at least partially, to the cold biases in the TNA?

By focusing on the global SST biases in CMIP5 climate models, *Wang et al*. [2013] pointed out a link between the cold bias in the TNA and the warm bias in the SEP. The purpose of the present paper is to demonstrate that the cold bias in the TNA does contribute to the warm bias in the SEP by performing sensitivity model experiments. In section 2, we describe the models and datasets used in this paper. The relationship between the TNA cold bias and the SEP warm bias in CMIP5 models is briefly reviewed and described in section 3. In section 4, we present the coupled ocean and atmosphere model response to the TNA cold SST bias. A short discussion and summary are given in section 5.

2. Coupled Models and Methods

This study is based on 22 coupled GCM output data of the "historical" simulations in CMIP5 [*Taylor et al*., 2012]. The modeling center, country and name are listed in Table S1 of the auxiliary material. The SST data from NOAA Extended Reconstruction Sea Surface Temperature version 3 (ERSST v3) is also used to validate the variability of coupled GCM simulations. We use the 106-year period of 1900-2006 to calculate the long term means.

To investigate the physical mechanism connecting the TNA and SEP SST biases, we conduct two sensitivity experiments by using the fully coupled NCAR Community Earth System Model (CESM1.0.4) [*Danabasoglu et al*., 2012]. The first experiment is the control relaxing run and named as REX_CTR. The ocean and atmosphere are fully coupled except in the TNA region where we relax the model-produced SST to the climatological SST of CESM1.0.4 at every integration step. Here the CESM1.0.4 climatological SST is obtained by averaging the last 100 years of 1500 years long-term fully coupled CESM1.0.4 simulation. The second experiment is configured the same as the first experiment but with the SST in the TNA region relaxing to the

CESM1.0.4 climatological SST added with the monthly SST cooling bias in the region of 0°N-30°N and from the east to west coast. This experiment is named as REX_TNAbias. Both the REX_CTR and REX_TNAbias experiments are integrated for 100 years. The difference averaged in the last 30 years between the REX_TNAbias and REX_CTR runs is taken as the response to the cold bias in the TNA.

3. Relationship between the TNA Cold Bias and SEP Warm Bias in CMIP5 Models

Before performing model experiments, we first briefly show the relationship of the TNA cold and SEP warm biases in CMIP5 climate models [*Wang et al.*, 2013]. The model simulations in CMIP5 models show a large cold SST bias in the TNA, with an ensemble mean amplitude up to 2.5°C (Fig. 1). This cold bias persists throughout the whole year without a significant seasonal variability. For the spatial structure, the TNA cold bias tilts northeastward to the eastern subtropics, which coincides with the trade wind location and the subduction path. It implies that this cold bias may be related to the latent heat bias as a result of the overestimated trade wind strength or associated with the bias in the subtropics which propagates southward due to the subduction or advection process. Here, we don't focus on the mechanisms of SST bias on a specific region such as the TNA in detail, which will be the subject of a future work. We focus on the SEP where a large warm SST bias exists in excessive of 2.5°C off the coast of Peru (Fig. 1). This warm bias extends northward to the south of the equator in the eastern tropical Pacific and northwestward to the equator around 100°W. Similar to the cold bias in the TNA, the SEP warm SST bias is significant in all models and occurs in all seasons.

To examine further the SST biases in the TNA and SEP, we plot these biases in a scatterplot format using 18 CMIP5 models. As shown in Fig. 2, the TNA cold bias is negatively correlated with the SEP warm bias in all seasons. It means that as a cold SST bias appears in the TNA, a warm SST bias occurs in the SEP. This inter-model negative correlation between the TNA and SEP SST biases has the higher values in summer and autumn, with a correlation up to -0.58 and -0.60, respectively. In contrast, the correlations are -0.41 in winter and -0.38 in spring. This interhemispheric SST bias relation shows a remarkable resemblance to the AWP-SEP teleconnection proposed by *Wang et al*. [2010], supporting the possibility that the SST bias in the SEP may be partially attributed to the remote effect of the large SST biases in the TNA.

We choose three models of highest SEP warm and TNA cold biases in summer as the large TNA-SEP dipole SST bias models (EC-EARTH, IPSL-CM5B-LR, and MRI-CGCM3), and three models of lowest SEP warm and TNA cold biases as the small TNA-SEP dipole SST bias models (CanESM2, MPI-ESM-LR, and MPI-ESM-P). The SST and 850mb wind differences between the large and small TNA-SEP dipole bias models are exhibited in Fig. S1a of the auxiliary material. As expected, there is a cold SST anomaly in excessive of 3°C over the TNA and a warm SST anomaly on the order of 2.5°C off the coast of Peru. The wind difference is characterized by an anticyclonic wind over the TNA in response to the cold SST, which is consistent with previous studies [*Wang and Enfield*, 2001; *Zhang and Wang*, 2012]. Note that the northeast wind branch is extremely strong, which extends to the eastern tropical Pacific, and induces northeasterly wind anomalies north of the equator, northerly cross-equatorial winds, and northwesterly winds (due to Coriolis force) south of the equator. This C-shape wind anomaly coincides well with the eastern Pacific north-south dipole SST pattern, suggesting an important role of the wind-evaporation-SST (WES) feedback. It is also confirmed by the surface latent heat flux difference which favors the SEP warm anomaly (not shown). The impact of the anomalous TNA cooling on the SEP can be further obtained by inspecting the difference between the velocity potential and divergent wind at 850mb, as displayed in Fig. S1b. It is clearly seen that the cold TNA is associated with divergent flow of the lower troposphere that crosses the equator into the SEP. That is, the anomalous Hadley-type circulation shows decent in the western TNA and ascent over the SEP. In view of the mean atmospheric circulation, the effect of the anomalous SST cooling in the TNA is to weaken the regional Hadley-type circulation from the TNA region to the SEP. This meridional circulation weakens the South Pacific subtropical anticyclone and the easterly trade winds near the equatorial eastern/central Pacific. The weakened easterly trade winds and subsidence eventually affect the SEP SST.

Note that the SST and wind differences are calculated between the large and small TNA-SEP dipole SST bias models, which may also include the effects of other variability in regions such as the tropical eastern south Pacific and Africa. Therefore, next we use the fully coupled CESM1.0.4 model experiments to demonstrate the influences associated with variability in the circulation due to the TNA cold bias.

4. Coupled Model Response to the TNA Cold SST Bias

The annual mean SST response in the eastern tropical Pacific is characterized by a north-south dipole, with the cold and warm anomaly north and south of the equator, respectively

(Fig. 3a). The magnitude of the SEP SST warm response is as high as 0.6°C, which accounts for 25%-30% of the SEP warming bias presented in Fig. 1. This suggests that the SST bias in the SEP is partially attributed to the remote effect of the cold SST biases in the TNA. In contrast to the SEP warm bias in CMIP5 models which is mainly confined east of 110°W, the modeling warm response in the SEP Ocean occupies a broad region, which extends northwestward from the coastal region into the central and western equator. This may be due to the positive effect of Bjerknes and WES feedbacks. The former tends to propagate the warm anomaly from the eastern Pacific to the western Pacific and the latter plays an important role for the warm SSTs propagating from the extratropics to the tropics.

The SEP warm SST anomaly can be generated as follows: The TNA cold bias suppresses convection and rainfall near the AWP region (Fig. 3b), producing a surface high extending to the eastern tropical North Pacific, a Rossby wave response (Fig. 3c). Over the eastern tropical Pacific, this anomalous high induces northeasterly wind anomalies north, northerly cross-equatorial winds, and northwesterly winds south of the equator (Fig. 3a). This C-shape wind anomaly generates a dipole SST anomaly (warm and cold south and north of the equator, respectively) through changes in evaporation. It appears that this coupled WES feedback, which has been extensively studied in relation to tropical Atlantic variability [*Xie and Carton*, 2004], acts to amplify the SST dipole. The northwesterly wind south of the equator also reduces the coastal upwelling, which also partly contributes to the SEP warm anomaly. The formation of cross-basin non-divergent wind is primarily due to the weakening of the Hadley-type circulation from the AWP region to the SEP as a result of the cold SST bias imposed in the TNA region. As exhibited in Figs. 4a and b, the TNA cooling is associated with a divergent circulation in the low troposphere that crosses the equator into the South Pacific and vice versa for the upper troposphere. This meridional circulation reduces the South Pacific subtropical anticyclone (Fig. 3c) and the associated subsidence, which in turn leads to a reduction of low clouds, a weakening of the easterly trade wind and thus an increase of the SST.

A heat budget analysis in the SEP region further confirms the physical mechanisms discussed above. It can be seen that the SEP warming is mainly associated with the surface heat flux heating (Fig. S2a of the auxiliary material), whereas the ocean dynamics play a damping role except in the southwestern coastal region (Fig. S2e). The positive contribution of heat flux arises from both the surface radiative and turbulent heat fluxes (Figs. S2b, c). The warm effect of radiative heat flux is dominant by the short wave radiation as a result of a reduction of low clouds (Fig. S2d). As discussed above, the regional Hadley-type circulation from the AWP region to the SEP is significantly weakened, leading to a reduction of the SEP subsidence, a decrease of the stratocumulus, and thus an increase of the downward shortwave radiation. The turbulent heat flux is primarily attributed to the latent heat flux due to the weakening of the trade wind (Fig. 3a), while the sensible heat flux is of secondary importance (not shown).

There are both local and remote atmospheric responses to the TNA cold bias. Here the baroclinic and barotropic streamfunctions are calculated as $\psi_c = (\psi_{850mb} - \psi_{250mb})/2$ and $\psi_t = (\psi_{850mb} + \psi_{250mb})/2$, respectively. As shown in Fig. 4d, the baroclinic streamfunction response shows a pair of anticyclones: one in the TNA and northeastern Pacific and the other in the SEP and South America. This model response is largely consistent with *Gill*'s [1980] solution to a cooling anomaly slightly north of the equator [*Heckley and Gill*, 1984]. Different from the atmosphere model response in *Wang et al*. [2010], there is also a strong pair of cyclones in the western Pacific. This can be interpreted as follows: the SEP warm anomaly gradually propagates to the western and central Pacific due to the positive Bjerknes and WES feedbacks, which induces a large amount of precipitation there (Figs. 3a, b). The heating anomaly over the western tropical Pacific eventually induces a baroclinic response represented by a pair of cyclones. In addition to the baroclinic response, the tropical Pacific warming also triggers the classical Pacific North America (PNA) pattern, which is largely barotropic [e.g., *Horel and Wallace*, 1981]. The PNA teleconnection is clearly seen from the barotropic streamfunction (Fig. 4c) and the geopotential height responses (Fig. S3).

Consistent with the atmosphere model responses in an AGCM [*Wang et al*., 2010] and in a simple atmospheric model [*Lee et al*., 2009], the barotropic component also shows a pattern of alternating high and low centers from the TNA to high latitudes (Fig. 4c). In response to the PNA teleconnection, the surface wind in the North Pacific Ocean is characterized by a cyclone, which generates a horseshoe-like SST pattern, with a cooling in the northwestern and central Pacific and a warming in the east extending northwest into the subpolar Ocean and southwest into the subtropics (Fig. 3a). This SST response is mainly due to the surface heat flux and temperature advection by the anomalous meridional current (not shown). The eastern warming is also propagated to the western tropics by the positive WES feedback as seen in other models [*Zhang et al*., 2011a, b], which in turn reinforces the tropical Pacific warming, the western Pacific baroclinic cyclones and the subsequent PNA teleconncetion. Therefore, the TNA cold bias not only induces SST response in the SEP, but also induces significant SST responses in the North Pacific. We also find that there is a close relationship between the TNA cold bias and the North Pacific cold bias in CMIP5 models. However, the purpose of present paper is only to focus on the remote effect of the TNA cold bias on the SEP warm bias. The remote effect on the North Pacific Ocean is beyond the scope of the present paper and will be explored in the future.

4. Discussions and Summary

The results presented here suggest that the SEP warm bias in coupled ocean-atmosphere models may come from two different sources: one is locally induced and the other is via remote processes. The leading candidates for the local influence are regional feedbacks between stratocumulus clouds, surface winds, upwelling, coastal currents and SST in the SEP region, which are poorly represented in many climate models. On the other hand, the SEP warm bias may contain a significant component that comes from the large biases in the TNA via remote processes. This remote effect can be seen in CMIP5 models: those models with colder TNA bias have warmer SEP bias, and vice versa. We use the numerical experiments of CESM1.0.4 to show that as much as 30% of the warm SST bias in the SEP can be attributed to the cold SST biases in the TNA. If this assessment is accurate, then the remote impact of the TNA biases is too significant to be ignored. This means that effort of reducing coupled model biases in the SEP should take into the consideration not only the local processes, but also the remote influence, especially in the TNA.

The detailed mechanism through which the TNA biases affect the SEP is briefly explored in this study. The cold bias in the TNA region weakens the Hadley-type circulation from the AWP region to the SEP. The TNA cooling is associated with a divergent (convergent) circulation in the low (upper) troposphere that crosses the equator into the South Pacific. This meridional circulation and the associated subsidence reduce the South Pacific subtropical anticyclone, and in turn lead to a reduction of low clouds, a weakening of the easterly trade wind and thus an increase of the SST. The present paper shows that the SEP can be remotely influenced by the TNA variability. This indicates that if models cannot succeed in stimulating the TNA variability, they will also fail at least partially over the SEP.

Acknowledgement

This work was supported by grants from National Oceanic and Atmospheric Administration (NOAA) Climate Program Office, the base funding of NOAA Atlantic Oceanographic and Meteorological Laboratory (AOML), National Science Foundation, and National Basic Research Program of China (2010CB950500 and 2013CB430301). The findings and conclusions in this report are those of the author(s) and do not necessarily represent the views of the funding agency.

References

Colbo, K., and R. A. Weller (2007), The variability and heat budget of the upper ocean under the Chile-Peru stratus. *J. Marine. Res.*, *65*, 607-637.

Danabasoglu, G., S. C. Bates, B. P. Briegleb, S. R. Jayne, M. Jochum, W. G. Large, S. Peacock and S. G. Yeager (2012), The CCSM4 Ocean Component. *J. Clim.*, *25*, 1361–1389.

Szoeke, De., P. Simon and S.-P. Xie (2008), The Tropical Eastern Pacific Seasonal Cycle: Assessment of Errors and Mechanisms in IPCC AR4 Coupled Ocean–Atmosphere General Circulation Models. *J. Clim.*, *21*, 2573–2590.

Gill, A.E., 1980: Some simple solutions for heat-induced tropical circulation. *Quart. J. Roy. Meteor. Soc.*, *106*, 447-462.

Heckley, W. A., and A. E. Gill (1984), Some simple analytic solutions to the problems of forced equatorial long waves. *Quart. J. Roy. Meteor. Soc.*, *110*, 203-217.

Horel, J. D., and J. M. Wallace (1981), Planetary-Scale atmospheric phenomena associated with the southern oscillation. *Mon. Wea. Rev.*, *109*, 813-829.

Huang, B., and E. K. Schneider (1995), The response of an ocean general circulation model to surface wind stress produced by an atmospheric general circulation model. *Mon. Wea. Rev.*, *123*, 3059–3085.

Lee, S.-K., C. Wang and B. E. Mapes (2009), A simple atmospheric model of the local and teleconnection responses to tropical heating anomalies. *J. Clim.*, 22, 272-284.

Ma, C.-C., C. R. Mechoso, A. W. Robertson, and A. Arakawa (1996), Peruvian stratus clouds and tropical Pacific circulation: a coupled ocean–atmosphere GCM study. *J. Clim.*, *9*, 1635–1645.

Meehl, G. A., C. Covey, B. McAvaney, M. Latif, and R. J. Souffer (2005), Overview of the coupled model intercomparison project. *Bull. Am. Meteorol. Soc.*, *86*, 89–93.

Mechoso, C. R. et al. (1995), The seasonal cycle over the tropical Pacific in Coupled

Ocean-Atmosphere General Circulation Models. *Mon. Wea. Rev.*, *123*, 2825-2838.

Schneider, E. K., Z. Zhu, B. S. Giese, B. Huang, B. P. Kirtman, J. Shukla, and J. A. Carton (1997), Annual cycle and ENSO in a coupled ocean–atmosphere model. *Mon. Wea. Rev.*, *125*, 680–702.

Taylor, K. E., R. J. Stouffer, and G. A. Meehl (2012), An overview of CMIP5 and the experiment design. *Bull. Amer. Meteor. Soc.*, *93*, 485-498.

Wang, C., L. Zhang, S.-K. Lee, C. R. Mechoso, L. Wu (2013), A global perspective on CMIP5 climate model biases, *Nature Climate Change*, revised.

Wang, C., S.-K. Lee, and C. R. Mechoso (2010), Interhemispheric influence of the Atlantic warm pool on the Southeastern Pacific. *J. Clim.*, *23*, 404-418.

Wang, C., and D. B. Enfield (2001), The tropical Western Hemisphere warm pool. *Geophys. Res. Lett.*, *28*, 1635-1638.

Xie, S.-P., and J. A. Carton (2004), Tropical Atlantic variability: Patterns, mechanism, and impacts. Earth Climate: The Ocean–Atmosphere Interaction. *Geophys. Monogr.*, *147*, 121–142.

Zhang, L., and C. Wang (2012), Remote influences on freshwater flux variability in the Atlantic warm pool region. *Geophys. Res. Lett.*, *39*, doi:10.1029/2012GL053530.

Zhang, L., L. Wu, and J. Zhang (2011a), Coupled Ocean-Atmosphere Responses to Recent Freshwater Flux Changes over the Kuroshio-Oyashio Extension Region. *J. Clim.*, *24*, 1507-1524.

Zhang, L., L. Wu, and J. Zhang (2011b), Simulated Response to Recent Freshwater Flux Change over the Gulf Stream and Its Extension: Coupled Ocean–Atmosphere Adjustment and Atlantic–Pacific Teleconnection. *J. Clim.*, *24*, 3971-3988.

List of Tables:

Table 1. The 18 models involved in this study and their sponsor, country, and names.

Figure Captions:

Figure 1. (a) Spring (MAM), (b) summer (JJA), (c) autumn (SON) and (d) winter (DJF) mean SST bias averaged in 18 CMIP5 models. Unit is ^{o}C. Here, the SST bias is calculated by subtracting the ERSST from the long term mean coupled model SST. The black boxes in (a) denote the regions for the scatterplot in Fig.2. The dotted region denotes 18 models have the same sign.

Figure 2. Scatterplot of the spring (a), summer (b), autumn (c) and winter (d) mean tropical North Atlantic SST bias (5^{o}N-25^{o}N, 70^{o}W-25^{o}W) versus southeastern Pacific SST bias (30^{o}S-5^{o}S, 100^{o}W-coast).

Figure 3. (a) SST (^{o}C) and wind stress (N/m^{2}), (b) precipitation (mm/day) and (c) sea level pressure (mb) differences between the REX_TNAbias and REX_CTRL runs.

Figure 4. (a) 850mb velocity potential ($10^{6}m^{2}s^{-1}$) and divergent wind (m/s), (b) 250mb velocity potential ($10^{6}m^{2}s^{-1}$) and divergent wind (m/s), (c) barotropic stream function ($10^{6}m^{2}s^{-1}$) and (d) baroclinic stream function ($10^{6}m^{2}s^{-1}$) differences between the REX_TNAbias and REX_CTRL runs.

Figure S1. (a) SST and 850mb wind differences between the large TNA-SEP dipole bias models (EC-EARTH, IPSL-CM5B-LR, and MRI-CGCM3) and the small TNA-SEP dipole bias models (CanESM2, MPI-ESM-LR, and MPI-ESM-P). (b) Same as (a) but for the 850mb velocity potential and divergent wind differences.

Figure S2. Heat budget analysis over the SEP region. (a) Net heat flux (W/m^2), (b) Radiative heat flux (W/m^2), (c) Turbulent heat flux (W/m^2), Low clouds (%), Ocean dynamics (W/m^2) and Vertical velocity at 50m (10^{-3} m/s) differences between the REX_TNAbias and REX_CTRL runs.

Figure S3. Geopotential height difference between the REX_TNAbias and REX_CTRL runs at (a) 850mb, (b) 500mb and (c) 250mb. Unit is m.

Table 1: The 18 models involved in this study and their sponsor, country, and names.

Sponsor, Country	Model Name
Commonwealth Scientific and Industrial Research Organisation (CSIRO) , Australia	ACCESS1.0
Canadian Center for Climate Modeling and Analysis, Canada	CanESM2
National Center for Atmospheric Research (NCAR), USA	CCSM4
Météo-France/Centre National de Recherches Météorologiques, France	CNRM-CM5
European Earth System Model,EU	EC-EARTH
U.S. Department of Commerce/National Oceanic and Atmospheric Administration (NOAA)/Geophysical Fluid Dynamics Laboratory (GFDL),USA	GFDL-CM3
	GFDL-ESM2G
	GFDL-ESM2M
Met office Hadley Centre, UK	HadCM3
	HadGEM2-CC
	HadGEM2-ES
Institute Pierre Simon Laplace, France	IPSL-CM5A-MR
	IPSL-CM5B-LR
Center for Climate System Research (University of Tokyo), National Institute for Environmental Studies, and Frontier Research Center for Global Change (JAMSTEC), Japan	MIROC5
Max Planck Institute for Meteorology, Germany	MPI-ESM-LR
	MPI-ESM-P
Meteorological Research Institute, Japan	MRI-CGCM3
Norwegian Climate Centre, Norway	NorESM1-M

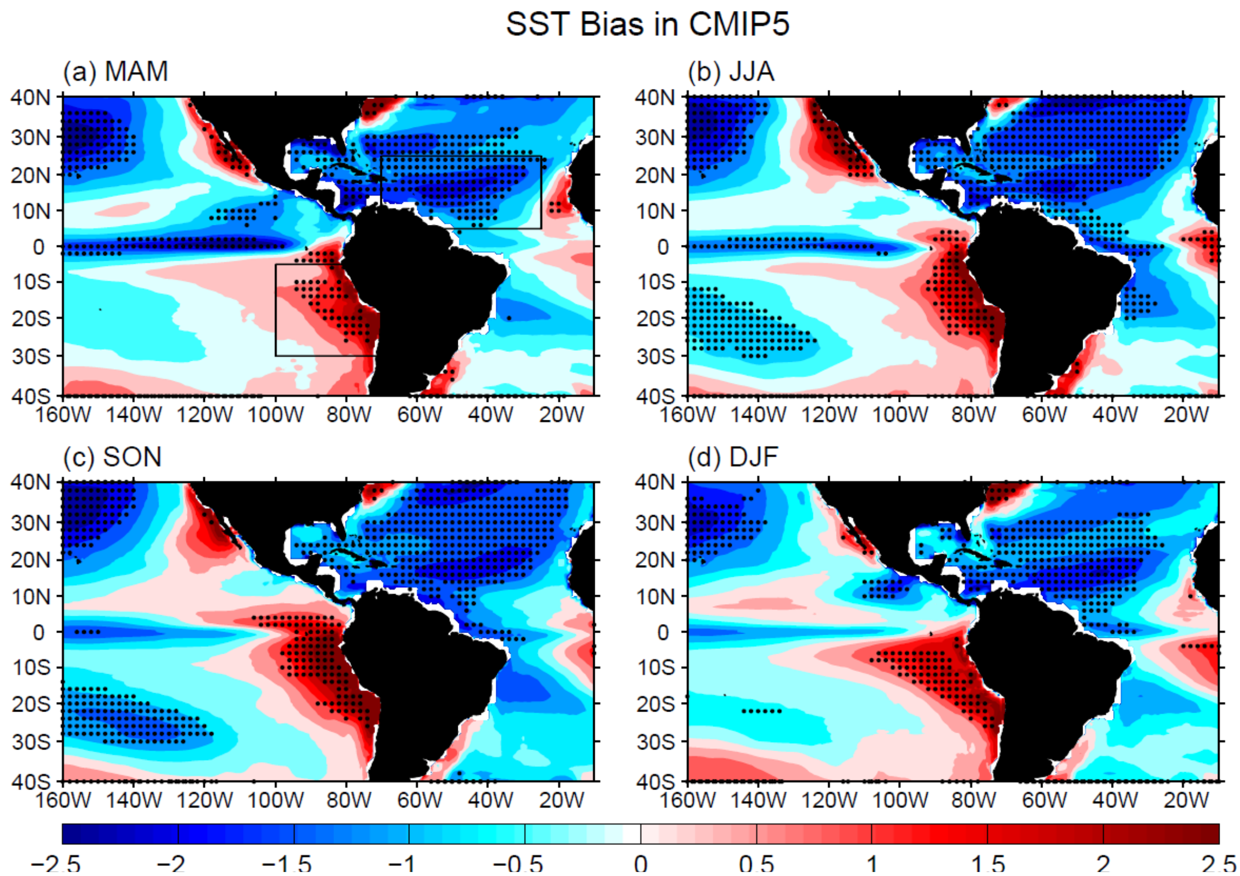

Figure 1. (a) Spring (MAM), (b) summer (JJA), (c) autumn (SON) and (d) winter (DJF) mean SST bias averaged in 18 CMIP5 models. Unit is °C. The SST bias is calculated by subtracting the ERSST from the long term mean coupled model SST. The black boxes in (a) denote the regions for the scatterplot in Fig. 2. The dotted region denotes that 18 models have the same sign.

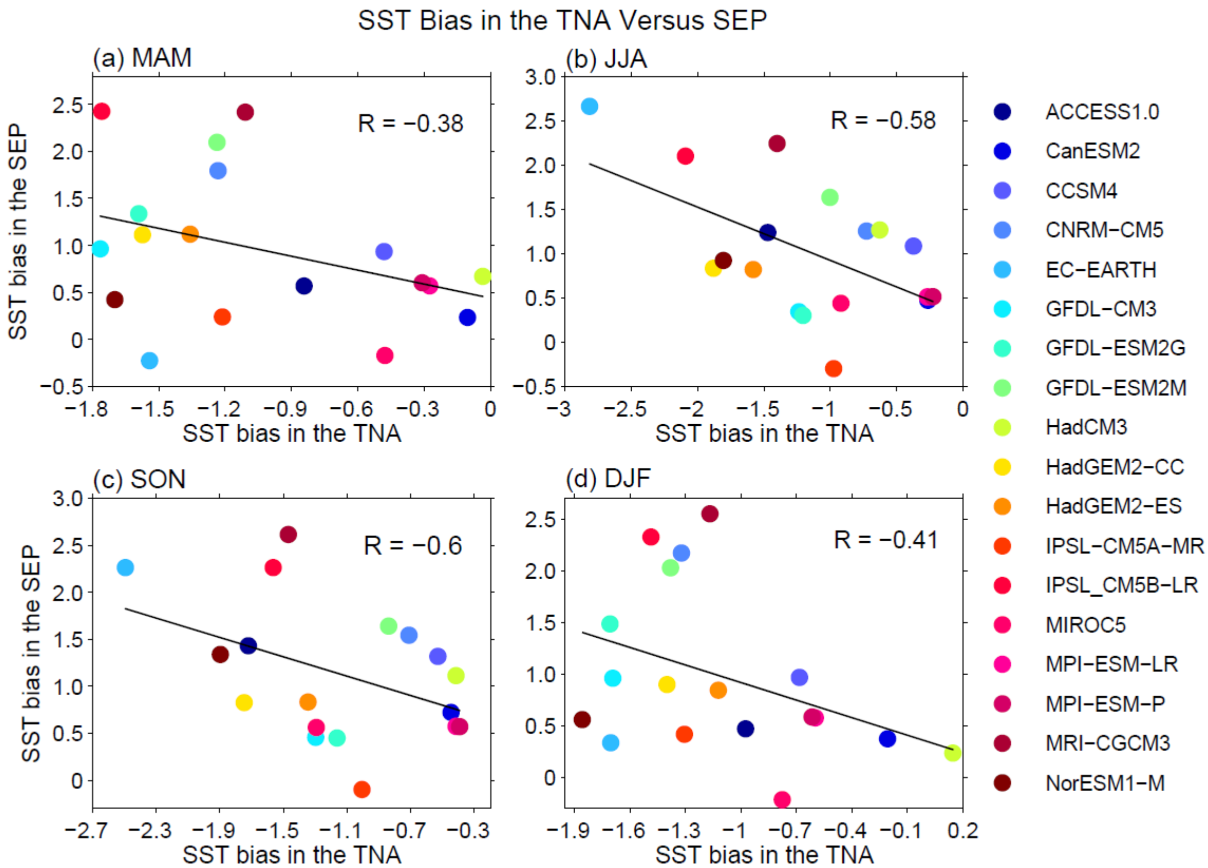

Figure 2. Scatterplot of the spring (a), summer (b), autumn (c) and winter (d) mean tropical North Atlantic SST bias (5°N-25°N, 70°W-25°W) versus southeastern Pacific SST bias (30°S-5°S, 100°W-coast).

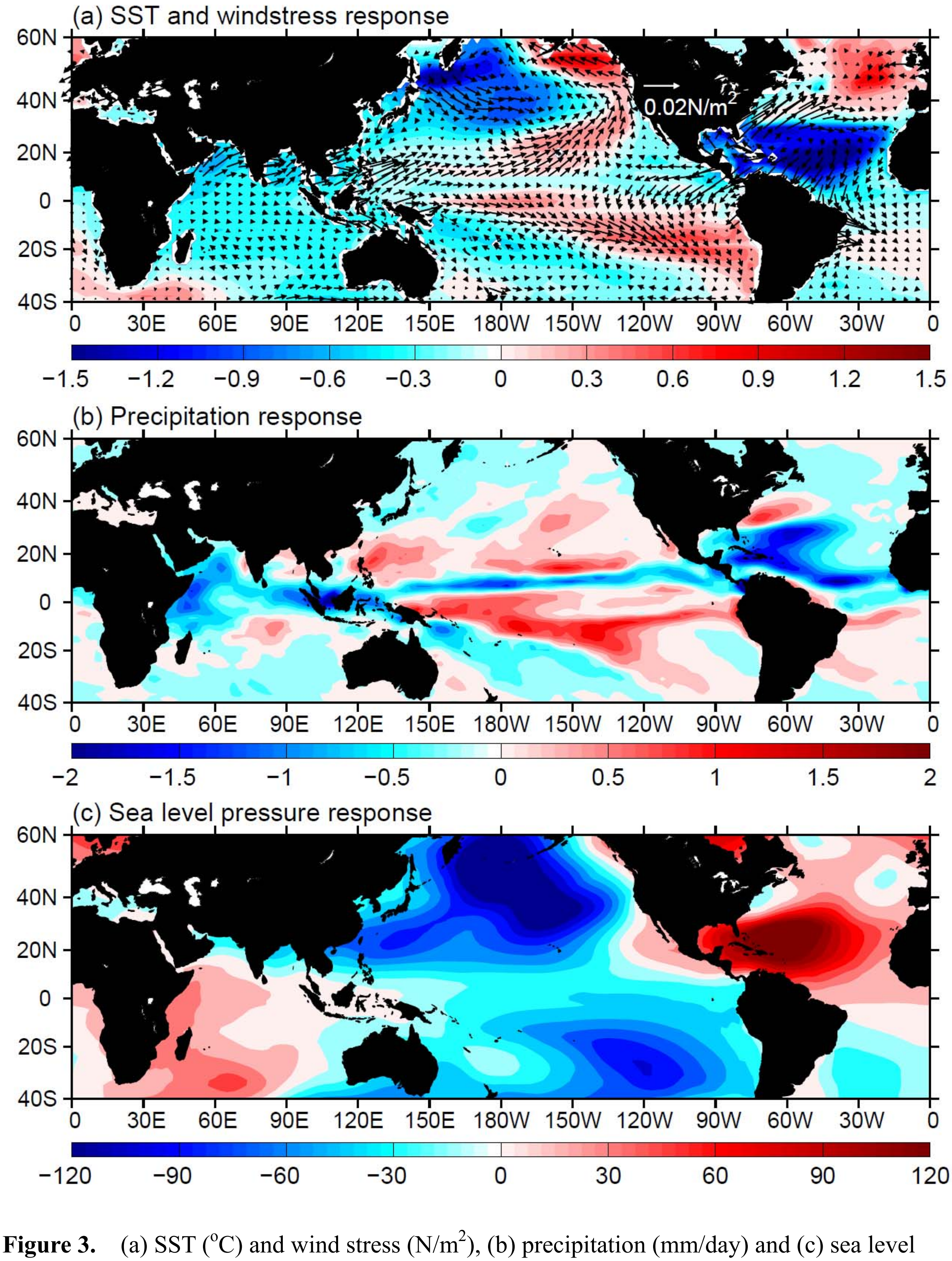

Figure 3. (a) SST (^oC) and wind stress (N/m^2), (b) precipitation (mm/day) and (c) sea level pressure (mb) differences between the REX_TNAbias and REX_CTRL runs.

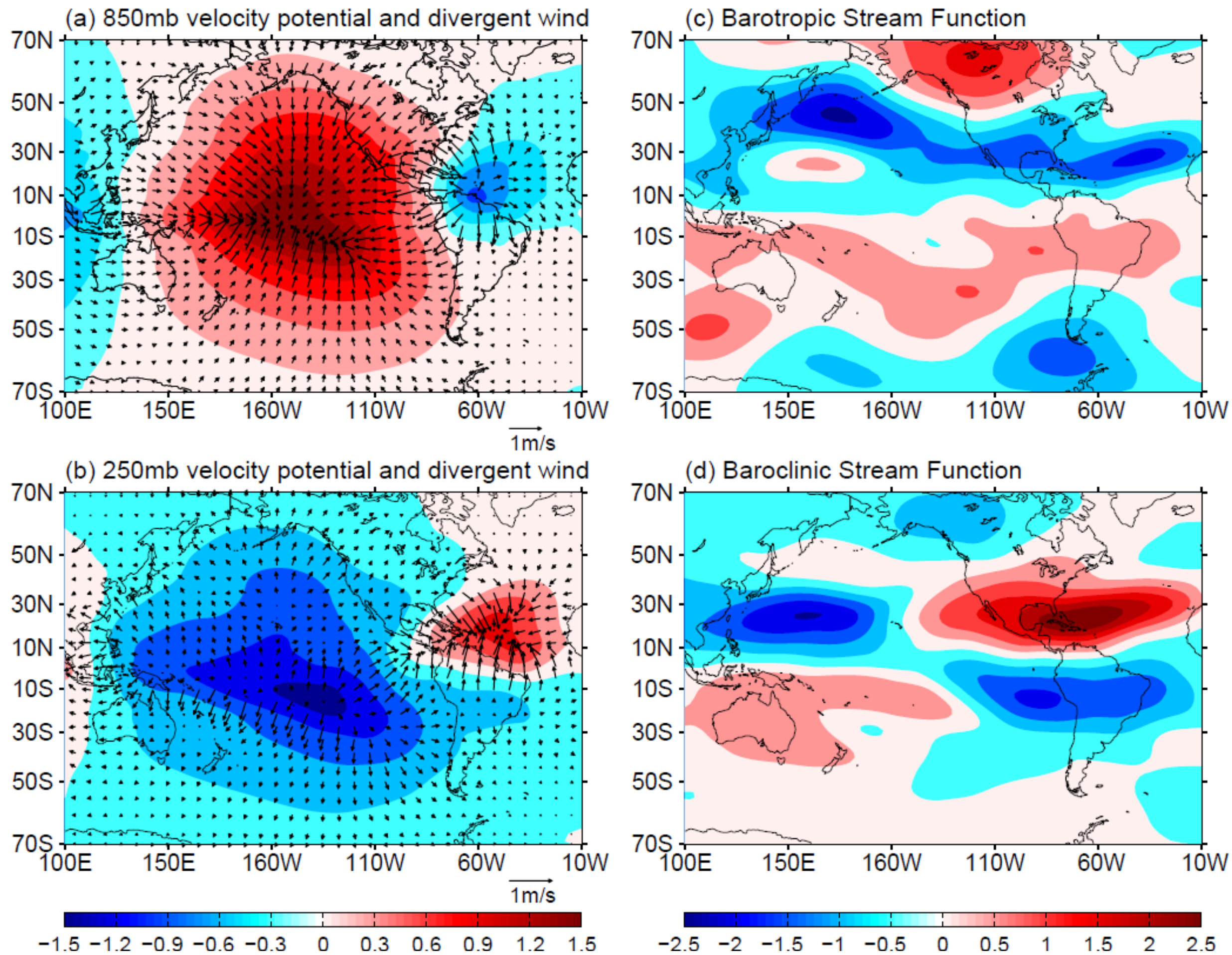

Figure 4. (a) 850mb velocity potential (10^6 m^2s^{-1}) and divergent wind (m/s), (b) 250mb velocity potential (10^6 m^2s^{-1}) and divergent wind (m/s), (c) barotropic stream function (10^6 m^2s^{-1}) and (d) baroclinic stream function (10^6 m^2s^{-1}) differences between the REX_TNAbias and REX_CTRL runs.

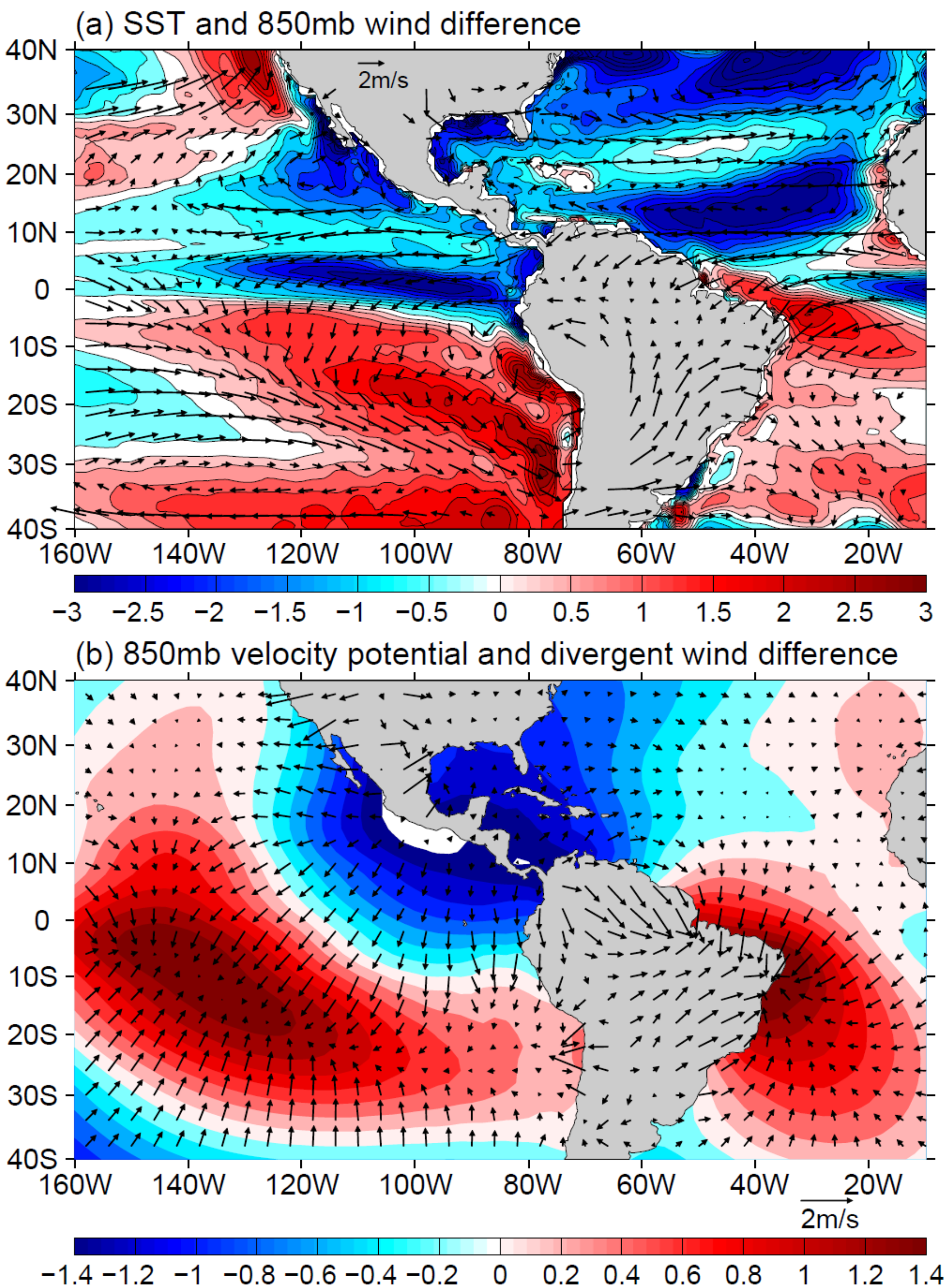

Figure S1. (a) SST and 850mb wind differences between the large TNA-SEP dipole bias models (EC-EARTH, IPSL-CM5B-LR, and MRI-CGCM3) and the small TNA-SEP dipole bias models (CanESM2, MPI-ESM-LR, and MPI-ESM-P). (b) Same as (a) but for the 850mb velocity potential and divergent wind differences.

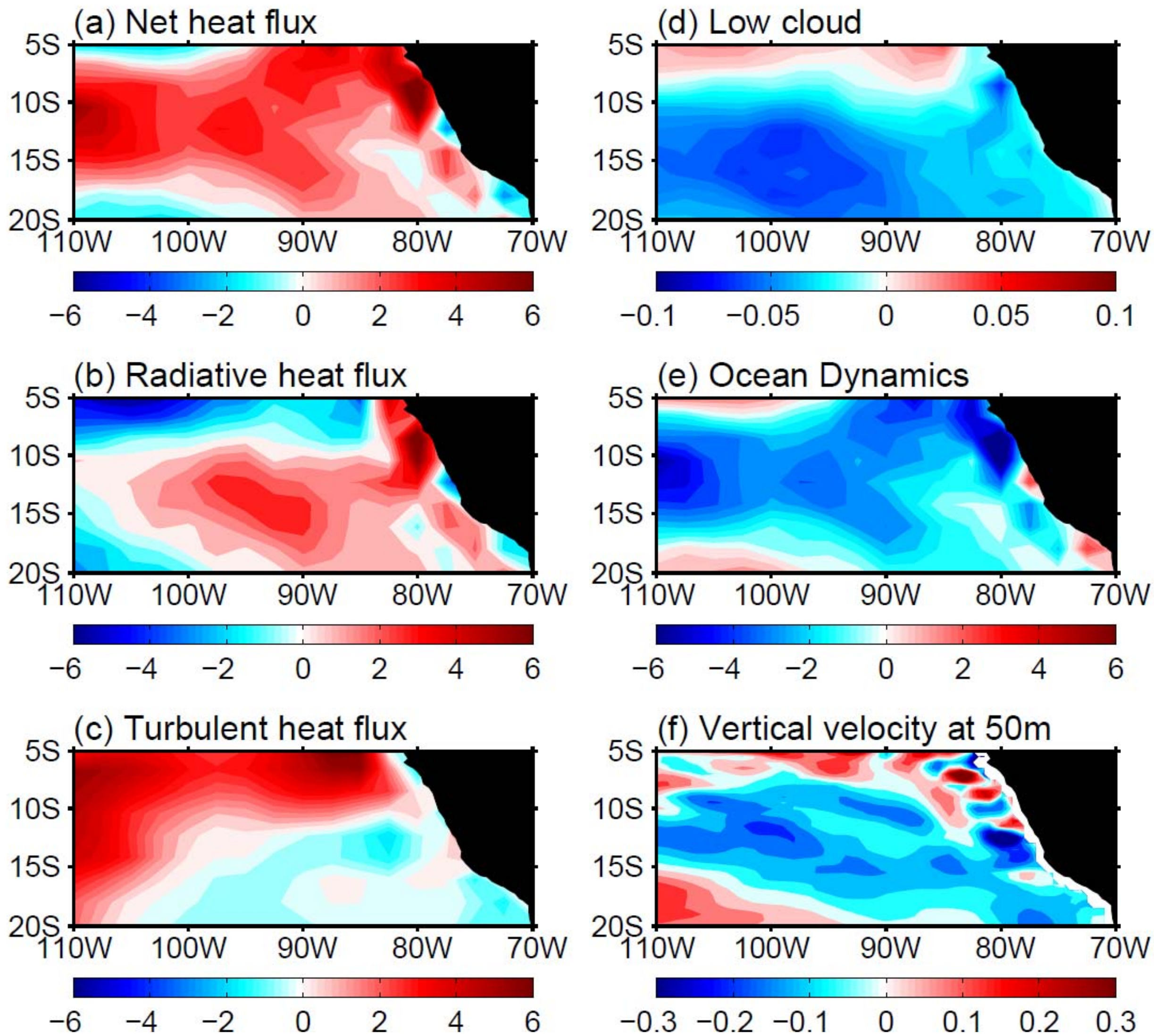

Figure S2. Heat budget analysis over the SEP region. (a) Net heat flux (W/m^2), (b) Radiative heat flux (W/m^2), (c) Turbulent heat flux (W/m^2), Low clouds (%), Ocean dynamics (W/m^2) and Vertical velocity at 50m (10^{-3} m/s) differences between the REX_TNAbias and REX_CTRL runs.

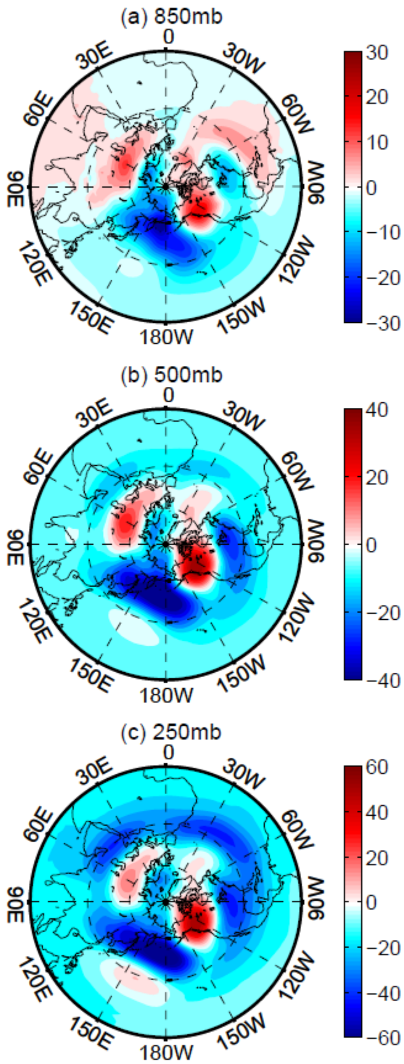

Figure S3. Geopotential height difference between the REX_TNAbias and REX_CTRL runs at (a) 850mb, (b) 500mb and (c) 250mb. Unit is m.